

Analysis of DCI Cask Drop Test onto Reinforced Concrete Pad

C.Ito, Y.Kato, S.Hattori, K.Shirai, M.Misumi, S.Ozaki

Nuclear Fuel Cycle Department
Central Research Institute of Electric Power Industry
1646 Abiko, Abiko-shi, Chiba-ken, 270-11 JAPAN

INTRODUCTION

In a cask-storage facility, a cask may be subjected to an impact load as a result of a free drop onto the floor because of cask mishandling. We performed drop tests of casks onto a reinforced concrete (RC) slab representing the floor of a facility as well as simulation analysis [Kato et al].

This paper describes the details of the FEM analysis and calculated results and compares them with the drop test results.

1. OUTLINE OF DROP TEST

We used three full-scale casks made of ductile cast iron for the drop tests. The casks were designed to accommodate 52 BWR-type spent-fuel assemblies; each cask was about 2-m diameter, 5-m long and weighted about 110 tons. Model spent-fuel assemblies equivalent to actual spent-fuel assemblies in dimensions and weight and dummy weights equivalent to actual spent-fuel assemblies in weight were used.

The specification of the RC slab was determined from the construction of the cask-storage facility designed in our previous study of spent-fuel storage facilities. The RC slab was 6-m wide, 6-m long, and 1.2-m thick.

The test conditions were determined by the drop orientation and height. The cask was dropped vertically, horizontally and obliquely.

The drop height was classified into three categories: On the basis of the normal operating height in the storage facility, on the basis of the maximum operating height in the storage facility, and to verify the cask margin handling conditions.

We carried out the drop tests without fitting an impact limiter because we were simulating casks in storage.

2. ANALYTICAL METHOD

2.1 Model of Concrete

(a) Stress-strain relationship

A Non-linear stress-strain relationship for concrete as shown in Fig. 1 was used for the hydrostatic pressure component of the stress. At loading and unloading, concrete has plastic behavior and elastic recovery, respectively.

(b) Compressive failure

The compressive failure criterion of this analysis takes the multiaxial stress condition [Ito et al] into account as shown in Fig. 2 on the assumption that concrete is a homogeneous and isotropic material.

The failure surface is expressed by octahedral stresses. The ultimate strength envelopes of the failure surface in the meridian plane are expressed by the following parabolic equations in terms of octahedral stresses on the basis of test results [Ohnuma, Ito].

$$\theta = 0^\circ : \frac{\tau_{oc}}{\sigma_c} = 0.0689 + 0.6868 \left(\frac{\sigma_{oct}}{\sigma_c} \right) - 0.0964 \left(\frac{\sigma_{oct}}{\sigma_c} \right)^2 \quad (1)$$

$$\theta = 60^\circ : \frac{\tau_{oc}}{\sigma_c} = 0.2040 + 0.8424 \left(\frac{\sigma_{oct}}{\sigma_c} \right) - 0.1204 \left(\frac{\sigma_{oct}}{\sigma_c} \right)^2 \quad (2)$$

where,

$$\sigma_{oct} = \frac{1}{3} (\sigma_1 + \sigma_2 + \sigma_3)$$

σ_c : compressive strength

$\sigma_1, \sigma_2, \sigma_3$: principal stress

The envelopes which are the intersection of ultimate strength surface and the deviatoric stress plane are given by the following expression.

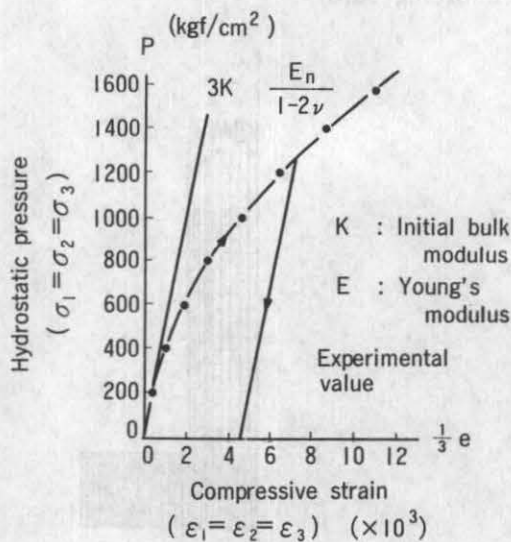


Fig. 1 Stress-Strain Relationship of Concrete under Hydrostatic Compression³

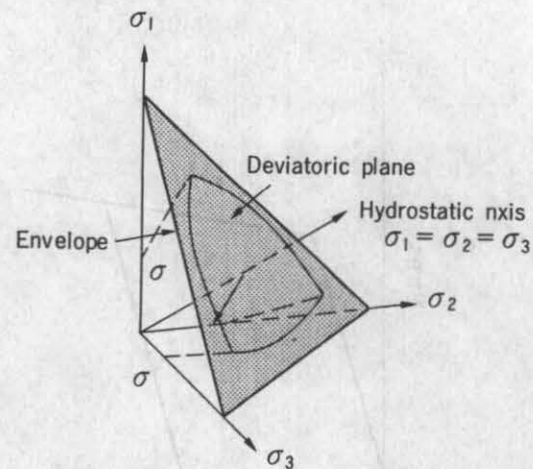


Fig. 2 Multi-Stress Condition

$$\tau_{oct}(\theta) = \frac{2\tau_{oct}(\tau_{oc}^2 - \tau_{oc}^2)\cos\theta + \tau_{oc}(2\tau_{oc} - \tau_{oc})\sqrt{4(\tau_{oc}^2 - \tau_{oc}^2)\cos^2\theta + 5\tau_{oc}^2 - 4\tau_{oc}\tau_{oc}}}{4(\tau_{oc}^2 - \tau_{oc}^2)\cos^2\theta + (\tau_{oc} - 2\tau_{oc})^2} \quad (3)$$

where,

τ_{oc} : Octahedral shear stress $\theta = 0^\circ$ calculated by Eq. (1)

τ_{oc} : Octahedral normal stress $\theta = 60^\circ$ calculated by Eq. (2)

$$\cos\theta = \frac{\sigma_1 + \sigma_2 - 2\sigma_3}{\sqrt{2\{(\sigma_1 - \sigma_2)^2 + (\sigma_2 - \sigma_3)^2 + (\sigma_3 - \sigma_1)^2\}}^{1/2}}$$

When the calculated octahedral shear stress exceeds τ_{oc} in Eq.(3), compressive failure is defined as occurring.

(c) Tensile failure criterion

Tensile failure occurs when one of the principal stresses exceeds the uniaxial tensile strength. The principal stress which exceeds the uniaxial tensile strength is defined as zero, and strains excluding real strains normal to the crack surface are recognized as the crack width. Consequently, the compressive stress in the direction normal to the crack does not yield until crack closure is recognized.

By using the above-mentioned procedures, this concrete tensile model can handle the directions and width of a crack in the concrete element.

2.2 Model of Reinforcing Bars

(a) Stress-strain relationship

The stress-strain relationship of reinforcing bars used in this analysis is shown in Fig. 3. It is a bilinear approximation and is based on the isotropic hardening rule.

(b) Failure criterion

The Von Mises yield criterion was applied to the reinforcing bars.

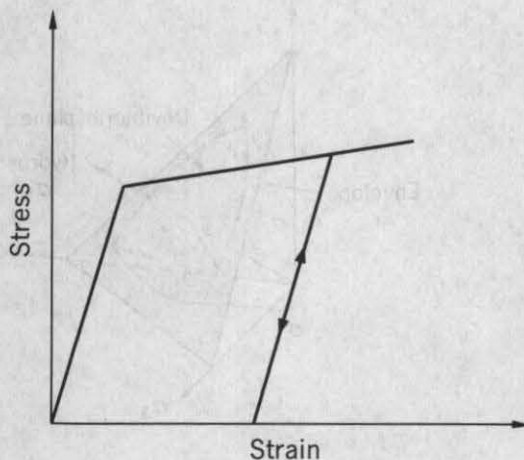


Fig. 3 Stress-Strain Relationship of Reinforcing Bars

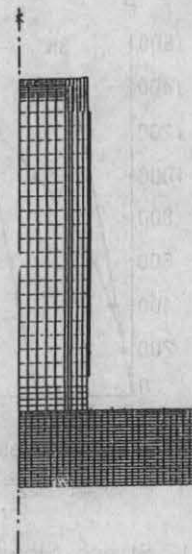


Fig. 4 Finite Element Model

2.3 RATE EFFECT

Deformation speed affects the characteristics of the mechanical properties such as yield stress of the material. In this analysis, the rate effect is given by:

$$\sigma_d / \sigma_s = f(\dot{\epsilon}(t))$$

where, σ_d is the dynamic strength of the material. σ_s is the static strength of the material and $\dot{\epsilon}$ is the strain rate. We applied this equation to each element of the model and at each step of the calculation.

3. RESULTS AND DISCUSSION

The calculation was carried for drop heights of 1.5 m, 7.5 m and 17.0 m in the vertical direction. The axisymmetrical model was applied in the analysis as shown in Fig. 4. The reinforcing-bar net was modeled by thin-shell elements which have the same reinforcement ratio as a real net of reinforcing bars.

Figures 5 through 8 compare the test results with the calculated results for accelerations and strains at the cask body and penetration depth of the slab. The calculated results are in good agreement with the test results and have an appropriate margin as shown in these figures.

Therefore, it seems that this analytical method can be applied to predict the behavior of a cask dropped onto an RC slab.

4. CONCLUSION

We validated the analytical code for an RC slab subjected to an impact load as a result of a free drop of a cask. Further study on calculation of the behavior of the RC slab is needed to establish a more accurate analytical method.

REFERENCE

- C.Ito et al.
Design Method of Reinforced Concrete Structure Against The Collision of Missile, CRIEPI REPORT, July 1991.
- Y.Kato et al.
Storage Cask Drop Test on Reinforced Concrete Slab, PATRAM'92, 1992.
- H.Ohnuma, C.Ito
Ultimate Strength Envelopes of Concrete under Triaxial Compressive Stresses, CAJ REVIEW, 1986.

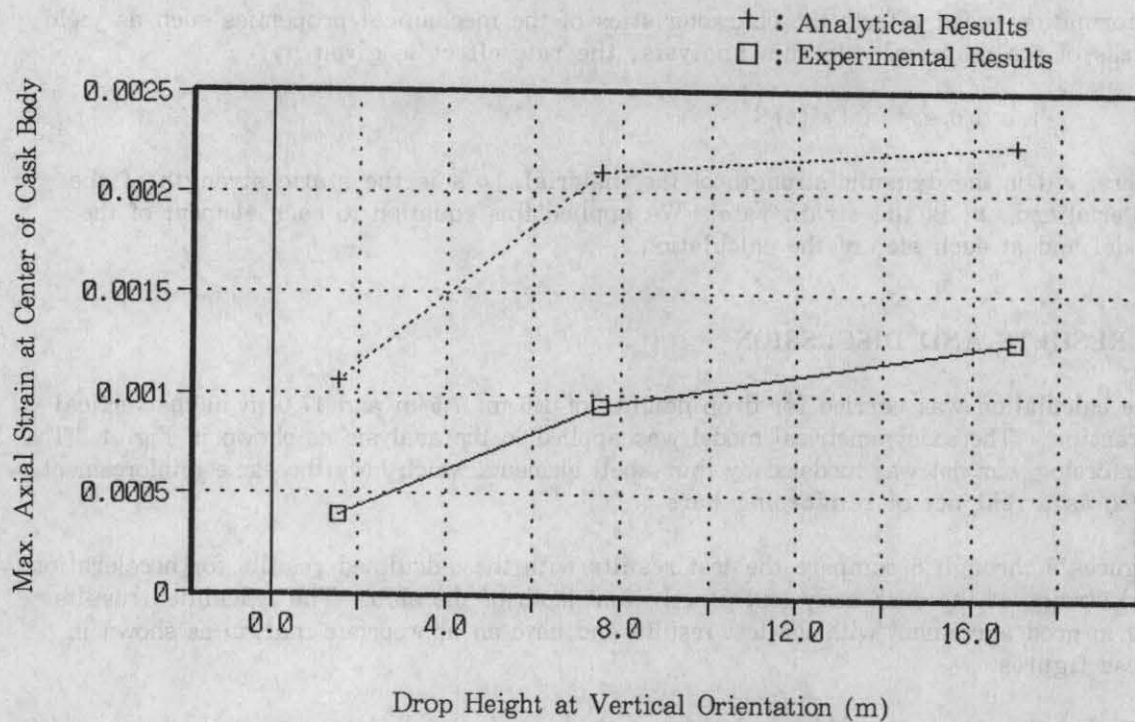


Fig. 5 Comparison Between Analytical and Experimental Results for Maximum Strain.

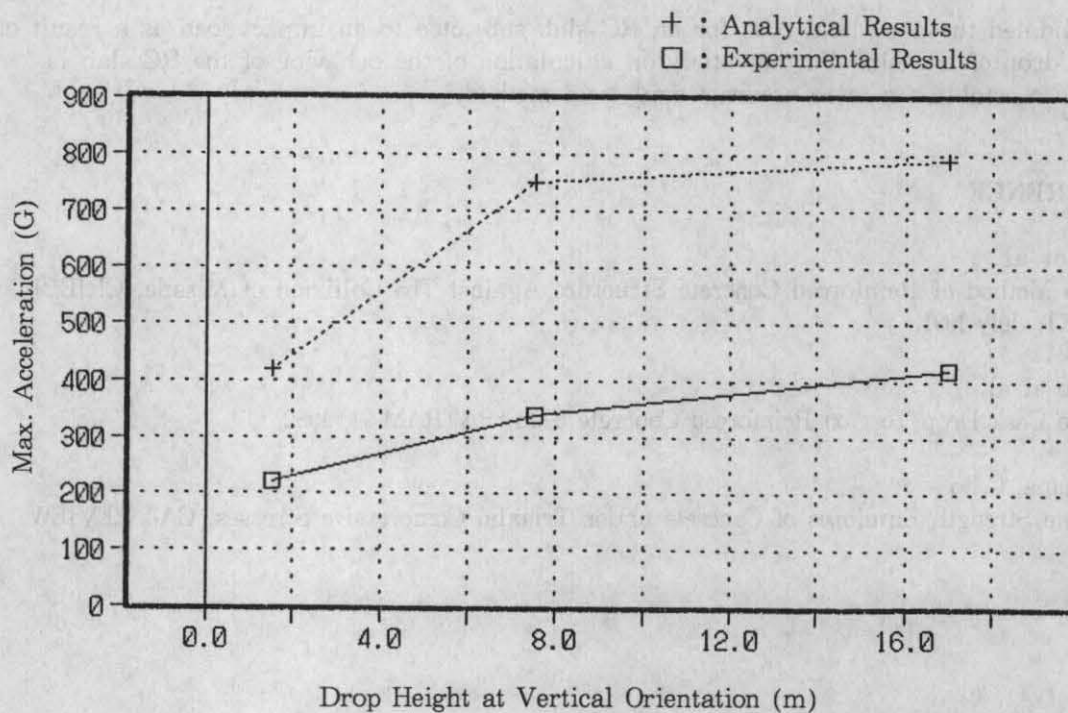


Fig. 6 Comparison Between Analytical and Experimental Results for Maximum Acceleration.

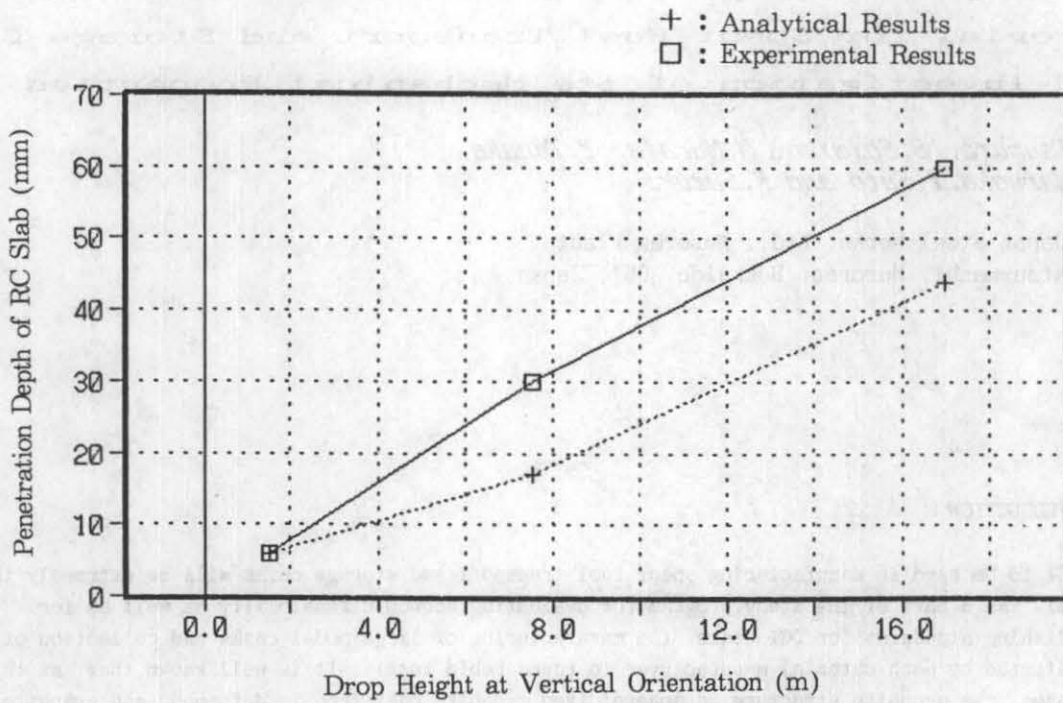


Fig. 7 Comparison Between Analytical and Experimental Results for Penetration Depth of RC slab.